

J.G. Leprince^{†1,5*}, G. Lamblin^{†1,2,5},
J. Devaux^{2,5}, M. Dewaele^{1,5},
M. Mestdagh^{3,5}, W.M. Palin⁶,
B. Gallez⁴, and G. Leloup^{1,5}

¹School of Dentistry and Stomatology, ²Laboratory of Chemistry and Physics of High Polymers, ³Interfacial Chemistry Laboratory, and ⁴Louvain Drug Research Institute, Biomedical Magnetic Resonance Unit, Université catholique de Louvain, Brussels, Belgium; ⁵CRIBIO (Center for Research and Engineering on Biomaterials), Avenue Hippocrate, 10/5721, B-1200 Brussels, Belgium; and ⁶Biomaterials Unit, University of Birmingham, College of Medical and Dental Sciences, School of Dentistry, St Chad's Queensway, Birmingham, B4 6NN, UK; [†]authors contributing equally to this work; *corresponding author, julian.leprince@uclouvain.be

J Dent Res 89(12):1494-1498, 2010

ABSTRACT

Different irradiation protocols are proposed to polymerize dental resins, and discordances remain concerning their impact on the material. To improve this knowledge, we studied entrapment of free radicals in unfilled Bis-GMA/TEGDMA (50:50 wt%) resin after light cure. The tested hypothesis was that various irradiation parameters (curing time, irradiance, and radiant exposure) and different irradiation modes (continuous and pulse-delay) led to different amounts of trapped free radicals. The analysis of cured samples ($n = 3$) by electron paramagnetic resonance (EPR) revealed that the concentrations of trapped free radicals significantly differed according to the curing protocol. When continuous modes with similar radiant exposure were compared, higher concentrations of trapped free radicals were measured for longer times with lower irradiance. Concerning pulse modes, the delay had no influence on trapped radical concentration. These results give new insights into the understanding of the photopolymerization process and highlight the relevance of using EPR when studying polymerization of dimethacrylate-based materials.

KEY WORDS: dimethacrylate resin, trapped free radicals, electron paramagnetic resonance, irradiation modes.

DOI:10.1177/0022034510384624

Received December 24, 2009; Last revision May 27, 2010; Accepted May 29, 2010

A supplemental appendix to this article is published electronically only at <http://jdr.sagepub.com/supplemental>.

© International & American Associations for Dental Research

Irradiation Modes' Impact on Radical Entrapment in Photoactive Resins

INTRODUCTION

In modern dentistry, photopolymerizable resin-based composites have become the choice material for the direct restoration of damaged teeth. However, despite significant material improvements since their introduction, several drawbacks—such as inadequate curing depths and deleterious effects of polymerization shrinkage stress—remain. In an attempt to overcome these deficiencies, various material aspects have been investigated, such as inorganic filler content, resin formulation, curing light technology, and photoinitiation protocols. In the latter field, despite the large number of studies analyzing the effects of various initiation modes on the properties of photoactive materials, discrepancies within the literature remain. Globally, two main goals are pursued. First, there exists a demand for reduction in curing exposure to minimize chairside procedure times of multi-increment resin composite restorations. Accordingly, several researchers support the exposure reciprocity law (Sakaguchi and Ferracane, 2001; Halvorson *et al.*, 2002; Price *et al.*, 2004; Emami and Söderholm, 2003), claiming that radiant exposure (RE , J/cm^2), the product of irradiance (I , mW/cm^2) and exposure time (t , s), is the main determining factor of the degree of conversion and mechanical properties of the photoactive material. This supposes reciprocity between I and t , and encourages a tendency among dentists and manufacturers to use or suggest a high-power illumination to reduce curing time. However, other studies (Musanje and Darvell, 2003; Asmussen and Peutzfeldt, 2005; Peutzfeldt and Asmussen, 2005; Dewaele *et al.*, 2009) have reported that although RE plays an important role, I and t independently influence polymer chain length, extent of crosslinking, and mechanical properties, and as such, exposure reciprocity does not hold under all conditions. Second, the use of “soft-start” curing protocols was proposed to delay the onset of polymer gelation. Notably, pulse-delay modes (consisting of a short flash of light, followed by a delay before the final polymerization) seem to contribute to a reduction of polymerization shrinkage stress (Kanca and Suh, 1999; Soh *et al.*, 2004; Chye *et al.*, 2005; Cunha *et al.*, 2008). Nevertheless, some authors have also highlighted lower conversion values and/or inferior mechanical properties of composites cured using those modes (Asmussen and Peutzfeldt, 2001, 2003; Lu *et al.*, 2005; Benetti *et al.*, 2007; Dewaele *et al.*, 2009). Although the use of alternative illumination methods may provide certain advantages, their effects on polymerization mechanisms and final polymer characteristics are poorly understood.

One interesting approach to a better grasp of the chemical process of photopolymerization is the observation of trapped free-radical concentration. It has been previously demonstrated that vitrified dental resins contain 2 types of trapped free radicals ($R^{\bullet}_{\text{Trapped}}$), which are detectable by electron paramagnetic resonance (EPR), namely, a “propagating” radical and an allylic radical type (Fig. 1) (Truffier-Boutry *et al.*, 2003). The study of $R^{\bullet}_{\text{Trapped}}$ is particularly relevant regarding dimethacrylate-based resins, since their polymerization leads to highly crosslinked networks, where monomolecular termination, as a consequence of radical entrapment, becomes the dominant pathway (Andrzejewska, 2001). A strong relationship between autoacceleration and radical trapping was also suggested (Zhu *et al.*, 1990). This highlights the importance of considering the quantity of trapped radicals in the study of the impact of photoirradiation protocols, which, to our knowledge, has never been investigated with clinically relevant irradiation parameters. For that reason, the aim of this paper was to test the null hypothesis that no difference in concentrations of $R^{\bullet}_{\text{Trapped}}$ existed between samples cured at similar *RE* but different *I* and *t*, with or without a delay.

MATERIALS & METHODS

Bisphenol A glycidyl dimethacrylate (Bis-GMA) (Heraeus Kulzer, Wehrheim, Germany) and triethylene glycol dimethacrylate (TEGDMA) (Aldrich, Belgium) were used without further purification from the supplier and mixed in a 50:50 wt% ratio. A photoinitiator system comprised of 0.5 mass% camphorquinone (CQ; Aldrich, Belgium) and 0.5 mass% of N,N-dimethyl-p-aminobenzoic acid ethyl ester (DABE, Aldrich) was incorporated into the resin. The resin was placed in a rectangular brass mould (7 x 1 x 1 mm), covered with Mylar film and cured (at $23 \pm 1^\circ\text{C}$) with a halogen light (Optilux 501, Demetron/Kerr Co., Orange, CA, USA) with the curing tip (8 mm exit diameter) centrally placed on the mould, in contact with the film. Two different illumination modes were used: continuous and pulse-delay (one-second cure, one- to two- or three-minute delay, final cure), for which *t* and *I* were adapted so that only 2 different *RE*s of 6 and 12 J/cm² were obtained (Table). A rheostat was used to achieve 3 specific irradiances (150, 300, and 600 mW/cm²) that were verified by differential scanning calorimetry (DSC822, Mettler Toledo, Zaventem, Belgium) equipped for *in situ* irradiation. An aluminum crucible filled with black graphite powder was irradiated to ensure complete absorption of emitted photons, while the other crucible was left empty and was not irradiated. Following irradiation, specimens (*n* = 3) were carefully stored in a lightproof container between subsequent measurements and recovered for analysis by EPR (MiniScope MS200 with rectangular resonator TE102, Magnostech, Berlin, Germany) 5 min, 1 to 6 hrs, 1 day, and 1, 2, and 3 mos post-irradiation. A similar EPR technique has been described in detail in other works (Ottaviani *et al.*, 1992; Sustercic *et al.*, 1997; Truffier-Boutry *et al.*, 2003, 2006). An alignment device was used to ensure an identical position of the sample in the EPR cavity, enabling accurate comparisons of the peak intensities to be made. EPR parameters consisted of: center field, 3367.42 G;

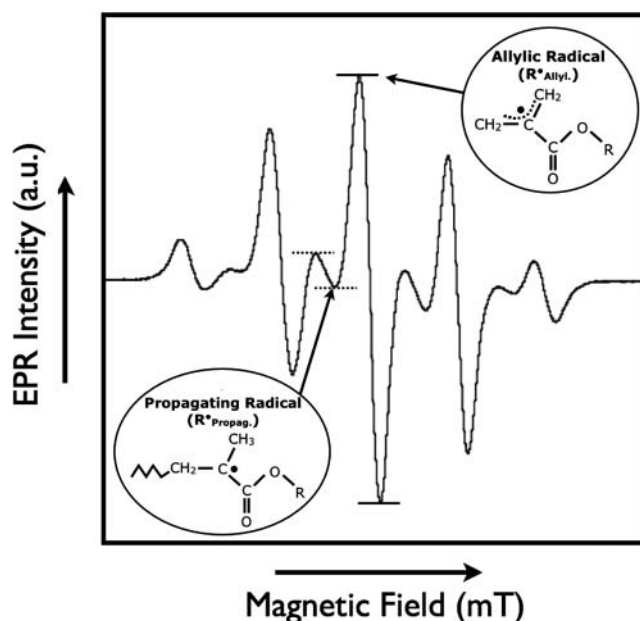


Figure 1. Nine-line EPR spectrum of experimental resin after polymerization and chemical structure of both radical species. *R* stands either for a pendant monomer, *i.e.*, Bis-GMA or TEGDMA, carrying the second and unreacted methacrylated group, or for a polymer chain. The respective intensities of both radical species were assessed by the measurement of peaks, indicated by arrows.

frequency, 9.30-9.55 GHz; sweep width, 198.40 G; modulation amplitude, 1 G; microwave power, 0.5 mW. Since peak width did not significantly vary with time, measurement of the height of some EPR peaks could be used to determine the relative concentrations of $R^{\bullet}_{\text{Trapped}}$: height of the fifth (from 334.9 to 335.5 mT) and fourth peaks (from 336.1 to 336.6 mT of the magnetic field) of the 9-line spectrum for allylic ($R^{\bullet}_{\text{Allyl}}$) and propagating radicals ($R^{\bullet}_{\text{Propag}}$), respectively (Fig. 1). These peaks are least influenced by the signal of the other radical types. Concentrations of $R^{\bullet}_{\text{Trapped}}$ (in arbitrary units, a.u.) at each storage time were analyzed by one-way ANOVA and Tukey’s test ($p = 0.05$).

RESULTS

The evolution of $R^{\bullet}_{\text{Trapped}}$ concentrations with time for the continuous modes for $R^{\bullet}_{\text{Allyl}}$ and $R^{\bullet}_{\text{Propag}}$, is presented in Figs. 2a and 2b, respectively. The curves of both radical species display similar profiles (logarithmic time scale), except during approximately the first 4 hrs, where concentrations of $R^{\bullet}_{\text{Propag}}$ decreased at higher rates compared with $R^{\bullet}_{\text{Allyl}}$, which is further highlighted in Fig. 2c. The curves are parallel during the first 24 hrs (Figs. 2a, 2b). Therefore, the results and statistical analyses for both radical types will be displayed only for five-minute and 24-hour storage periods (Table). In the same way, since pulse-mode curves showed profiles similar to continuous-mode curves, but overlapped with them, they were not displayed here for more clarity. Nevertheless, values and statistical analyses that were not reported in the manuscript are available in the

Table. Concentrations of Allylic and Propagating Radicals 5 min and 24 hrs after Photopolymerization

Modes	Radiant Exposure (J/cm ²)	Trapped Radical Concentrations (a.u.)				DC (%; mean ± SD)*
		Allylic Radicals		Propagating Radicals		
		5 min (mean ± SD)	24 hrs (mean ± SD)	5 min (mean ± SD)	24 hrs (mean ± SD)	
80 sec x 150 mW/cm ²	12	20353 (496) ^a	15933 (227) ^a	2049 (44) ^a	1327 (20) ^a	71 (2.0)
40 sec x 300 mW/cm ²	12	17393 (498) ^b	13372 (302) ^{b,c}	1758 (68) ^b	1135 (37) ^{b,c,d}	72 (3.3)
1 sec - (1 min) – 39 sec x 300 mW/cm ²	12	17456 (531) ^b	13779 (315) ^b	1678 (28) ^{b,c}	1178 (28) ^{a,b,c}	63 (1.8)
1 sec - (2 min) – 39 sec x 300 mW/cm ²	12	17629 (439) ^b	14271 (106) ^b	1753 (56) ^b	1189 (15) ^{a,b}	64 (3.2)
1 sec - (3 min) – 39 sec x 300 mW/cm ²	12	17402 (808) ^b	13341 (575) ^{b,c}	1730 (89) ^{b,c}	1122 (32) ^{b,c,d}	66 (1.8)
20 sec x 600 mW/cm ²	12	16039 (114) ^{b,c,d,e}	12106 (500) ^{d,e}	1582 (22) ^{b,c,d}	1037 (52) ^{b,c,d,e,f,g}	69 (7.4)
1 sec - (1 min) – 19 sec x 600 mW/cm ²	12	16470 (225) ^{b,c,d}	12317 (225) ^{c,d,e}	1556 (170) ^{b,c,d,e}	1035 (15) ^{c,d,e,f,g}	65 (2.5)
1 sec - (2 min) – 19 sec x 600 mW/cm ²	12	16800 (278) ^{b,c}	12567 (236) ^{c,d}	1589 (59) ^{b,c,d}	1089 (40) ^{b,c,d,e}	65 (0.8)
1 sec - (3 min) – 19 sec x 600 mW/cm ²	12	15636 (76) ^{c,d,e,f}	11483 (76) ^{d,e,f}	1519 (148) ^{b,c,d,e}	996 (110) ^{d,e,f,g,h}	65 (4.2)
40 sec x 150 mW/cm ²	6	16288 (274) ^{b,c,d,e}	12440 (336) ^{c,d}	1714 (59) ^{b,c}	1069 (31) ^{b,c,d,e,f}	69 (2.9)
20 sec x 300 mW/cm ²	6	14792 (659) ^{e,f,g}	11199 (548) ^{e,f}	1546 (76) ^{b,c,d,e}	957 (54) ^{e,f,g,h}	68 (2.6)
1 sec - (1 min) – 19 sec x 300 mW/cm ²	6	13947 (894) ^{g,h}	10762 (487) ^{f,g,h}	1499 (59) ^{c,d,e,f}	925 (50) ^{f,g,h,i}	62 (1.5)
1 sec - (2 min) – 19 sec x 300 mW/cm ²	6	15145 (783) ^{d,e,f,g}	11424 (475) ^{d,e,f}	1615 (103) ^{b,c}	1017 (23) ^{d,e,f,g}	63 (0.4)
1 sec - (3 min) – 19 sec x 300 mW/cm ²	6	14373 (895) ^{f,g}	10854 (524) ^{f,g}	1495 (52) ^{c,d,e,f}	954 (35) ^{e,f,g,h}	61 (1.3)
10 sec x 600 mW/cm ²	6	12477 (198) ^{h,i}	9900 (20) ^{g,h,i}	1306 (33) ^{e,f,g}	850 (24) ^{h,i}	65 (0.5)
1 sec - (1 min) – 9 sec x 600 mW/cm ²	6	11994 (170) ⁱ	9565 (165) ^{h,i,i}	1348 (79) ^{d,e,f,g}	864 (34) ^{h,i}	60 (4.0)
1 sec - (2 min) – 9 sec x 600 mW/cm ²	6	11218 (579) ⁱ	8594 (553) ⁱ	1158 (80) ^g	792 (74) ⁱ	61 (3.9)
1 sec - (3 min) – 9 sec x 600 mW/cm ²	6	11747 (458) ⁱ	8799 (612) ^{i,i}	1289 (89) ^g	900 (93) ^{g,h,i}	61 (1.1)

Similar letters connect values that are not significantly different.

*Data from Dewaele *et al.*, 2009.

Appendix. In the Table is also reported the mean degree of conversion of each mode (published data from Dewaele *et al.*, 2009; data were obtained with the same resin and same irradiation protocols, and are reproduced here for reader convenience). Generally, increased concentrations of R_{Trapped}• were measured for continuous mode curing regimes following higher (12 J/cm²) compared with lower RE (6 J/cm²) (Figs. 2a, 2b, Table). However, the amounts of R_{Trapped}• generated by 20 sec x 600 mW/cm² (12 J/cm²) and 40 sec x 150 mW/cm² (6 J/cm²) were not significantly different (p > 0.05). Moreover, while the increase in concentrations of both radicals is significant (p < 0.05) at twice the exposure time (40 sec x 150 mW/cm² to 80 sec x 150 mW/cm² and 20 sec x 300 mW/cm² to 40 sec x 300 mW/cm²), it is not significant (p > 0.05) at twice the irradiance (40 sec x 150 mW/cm² to 40 sec x 300 mW/cm² and 20 sec x 300 mW/cm² to 20 sec x 600 mW/cm²). When continuous modes

with similar RE were compared, higher concentrations of R_{Trapped}• were measured for longer exposure time with lower irradiance. There was no influence of the delay time on the concentration of R_{Trapped}• for either the application of a one-, two-, or three-minute delay or when pulse delay was compared with continuous mode for the same RE (Table).

DISCUSSION

The two distinct phases of radical concentration, highlighting the decrease of R_{Trapped}• following polymerization, are in accordance with previous work (Truffier-Boutry *et al.*, 2006; Leprince *et al.*, 2009). The decrease in R_{Trapped}• from 0 to 24 hrs was attributed to post-cure volumetric shrinkage (Truffier-Boutry *et al.*, 2006), whereas from 24 hrs to 3 mos, the effect of oxidation by atmospheric oxygen may play a more significant role in the

reduction of radical concentration (Leprince *et al.*, 2009). Since 2 radical species are considered, the relationship between both species requires clarification. R_{Propag} concentrations decrease at higher rates than R_{Allyl} during the first 4 hrs. As mentioned above, during approximately the first 24 hrs after light cure, volumetric shrinkage occurs. As a result, R_{Trapped} move closer to each other, and the probability of termination increases due to shrinkage (Truffier-Boutry *et al.*, 2006). But while R_{Allyl} are unable to react with species other than free radicals (higher stability due to a resonance phenomenon), R_{Propag} exhibit sufficient reactivity to interact also with remaining double-bonds. In this way, additional propagation reactions can repeat locally, slightly increasing DC (Truffier-Boutry *et al.*, 2006) and local radical mobility, leading to some bimolecular radical termination through a reaction-diffusion-controlled termination mechanism (Anseth *et al.*, 1995). The different behaviors of the 2 different radical species observed here are an additional proof in favor of the identification of R_{Trapped} proposed by Truffier-Boutry *et al.* (2003). Previous work (Ottaviani *et al.*, 1992) also identified an EPR spectrum similar to that presented in Fig. 1, although in that study the signal disappeared several mos after irradiation, and other signals were detected in some commercial composites. Since unfilled experimental resins were tested in the present study, it could be hypothesized that fillers or other components of commercial resins may be responsible for the creation of additional minor signals.

Regarding the comparison of free-radical concentrations, the period from 5 min to 1 day post-cure should be considered, since radical concentration within this timeframe remains proportional between curing regimes. For continuous curing modes, the increase in R_{Trapped} concentration following twice the RE , by doubling either I or t , can be explained by the creation of a higher concentration of free radicals (generated by an increase in number of photons), which are more likely to become trapped. However, for similar RE , higher concentrations of R_{Trapped} were measured for longer t and lower I . This observation is in apparent contradiction to the reciprocity observed between I and t for CQ quantum yield of conversion (number of converted photoinitiator molecules *per* number of absorbed photons) (Chen *et al.*, 2007). However, even if the same total amount of radicals is created, it does not necessarily result in the same number entrapped. This can be explained by a consideration of both types of termination mechanisms co-existing during polymerization (Lovell *et al.*, 1999): While bimolecular termination probably prevails during the very initial stages of the reaction, monomolecular termination (first-order) dominates when molecular diffusion becomes limited (auto-acceleration). There is probably a loss of a given amount of radicals during the early stages by bimolecular termination. This loss (or early termination) is higher for high-irradiance protocols, since termination is proportional to $[R_{\text{Allyl}}]^2$. As a result, at constant RE but higher I and shorter t , the amount of growth centers created during auto-acceleration is lower, leading to a lower final concentration of R_{Trapped} . In other words, the amount of R_{Trapped} measured in the present work may provide an indication of the quantity of growth centers created during auto-acceleration. In light of these results, the use of EPR to measure R_{Trapped} gives

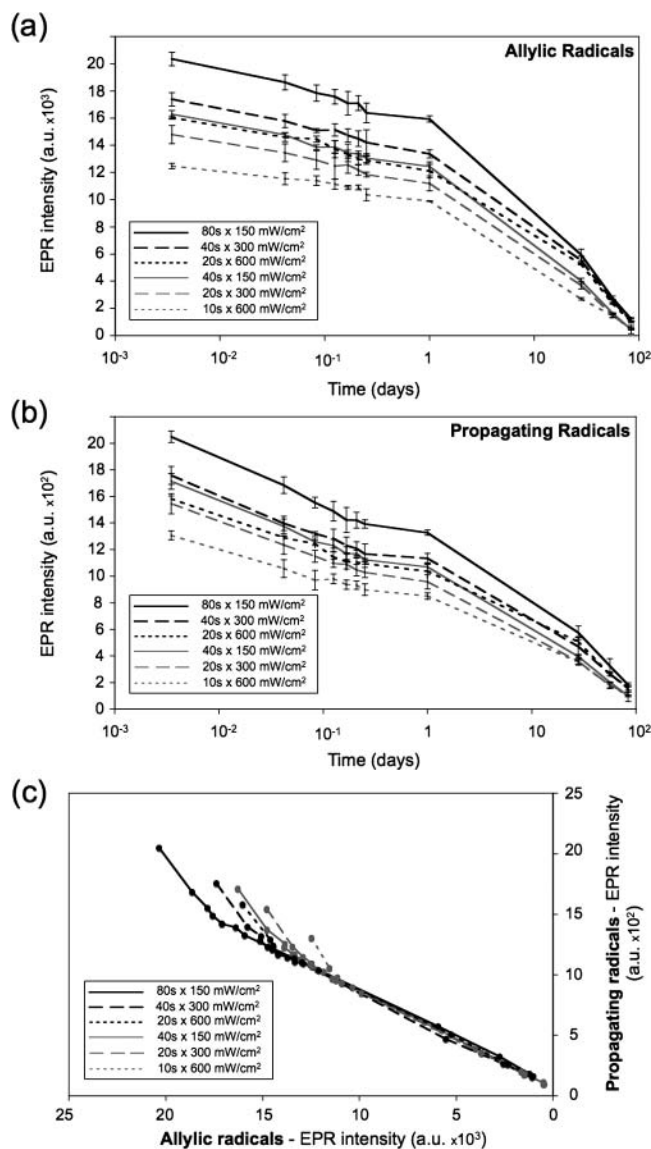


Figure 2. Concentration (in a.u., $n = 3$) of allylic radical (a) and propagating radical (b) as a function of time (means \pm SD at 5 min, 1 to 6 hrs, 1 day, and 1 to 3 mos—logarithmic scale) or 1 radical species as a function of the other (c) for continuous modes. Because of similar but overlapping profiles, pulse-mode curves are not displayed here, for more clarity. Black lines represent modes of 12 J/cm² and gray lines modes of 6 J/cm². In (c), each point indicates the respective concentrations of both radical types at a given time.

valuable information on monomolecular termination, which is critical in highly crosslinked systems. Other recent work has suggested that the applicability of exposure reciprocity law depends on factors other than irradiation parameters alone, such as the Bis-GMA/TEGDMA ratio (Feng and Suh, 2007). Besides, the efficiency of the photoinitiator or the amounts and types of inorganic fillers can also play a part in the resin reactivity, which can also result in different concentrations of R_{Trapped} . For example, previous work has demonstrated that the concentration of R_{Trapped} is about 3 times higher in the organic fraction of a filled

resin than in an unfilled resin of similar composition (Leprince *et al.*, 2009). As a consequence, the influence of filler content, monomer ratio, and photoinitiator might explain differences in previous results on commercial composites obtained by a similar EPR technique (Ottaviani *et al.*, 1992). Accordingly, the measurement of $R_{\text{Trapped}}^{\bullet}$ will be very useful in further understanding the impact of resin, photoinitiator chemistry, and filler morphology on complex photopolymerization processes, and related experiments are ongoing by the authors.

For pulse-delay modes, no influence of any delay time (1, 2, or 3 min with no irradiation) was observed on the concentration of $R_{\text{Trapped}}^{\bullet}$ or compared with continuous mode curing with similar *RE*. However, DC values associated with pulse-delay protocols were lower than those associated with the continuous mode of similar *RE* (Dewaele *et al.*, 2009), which can be explained by differences in polymer chain growth. The initial pulse probably results in microgels with relatively linear polymer chains (few pendant double-bonds available) (Poshusta *et al.*, 2002; Dewaele *et al.*, 2009) and where most free radicals probably terminated. During final irradiation, these microgel regions, in which unreacted double-bonds are less available, are certainly less reactive. Therefore, they may disturb the polymerization reaction compared with a continuous irradiation, leading to reduced DC. However, as discussed above, most of the free radicals are trapped when propagation becomes diffusion-controlled. Therefore, it might be assumed that the irradiation parameters at the time of auto-acceleration govern the final amount of trapped radicals, leading to comparable amounts of $R_{\text{Trapped}}^{\bullet}$ with or without a delay.

In conclusion, for continuous modes, the null hypothesis must be rejected, since the concentrations of $R_{\text{Trapped}}^{\bullet}$ between samples depend not only on *RE* but also on *I* and *t*. Conversely, regarding pulse-delay mode, the null hypothesis cannot be rejected, since the presence of a delay does not have a significant influence on the concentrations of $R_{\text{Trapped}}^{\bullet}$ when compared with the equivalent continuous mode of the same irradiance and total irradiation time.

ACKNOWLEDGMENTS

J. Leprince thanks the Belgian National Funds of Scientific Research (FNRS) for his fellow researcher position. Some of the present results were presented (abstract 1789) at the IADR General Session in Toronto, ON, Canada (2008).

REFERENCES

Andrzejewska E (2001). Photopolymerization kinetics of multifunctional monomers. *Prog Polym Sci* 26:605-665.

Anseth KS, Newman SM, Bowman CN (1995). Polymeric dental composites: properties and reaction behavior of multimethacrylate dental restorations. *Adv Polym Sci* 122:177-217.

Asmussen E, Peutzfeldt A (2001). Influence of pulse-delay curing on softening of polymer structures. *J Dent Res* 80:1570-1573.

Asmussen E, Peutzfeldt A (2003). Two-step curing: influence on conversion and softening of a dental polymer. *Dent Mater* 19:466-470.

Asmussen E, Peutzfeldt A (2005). Polymerization contraction of resin composite vs. energy and power density of light-cure. *Eur J Oral Sci* 113:417-421.

Benetti AR, Asmussen E, Peutzfeldt A (2007). Influence of curing rate of resin composite on the bond strength to dentin. *Oper Dent* 32:144-148.

Chen YC, Ferracane JL, Prah SA (2007). Quantum yield of conversion of the photoinitiator camphorquinone. *Dent Mater* 23:655-654.

Chye CH, Yap AU, Laim YC, Soh MS (2005). Post-gel polymerization shrinkage associated with different light curing regimens. *Oper Dent* 30:474-480.

Cunha LG, Alonso RC, Pfeifer CS, Correr-Sobrinho L, Ferracane JL, Sinhoreti MA (2008). Contraction stress and physical properties development of a resin-based composite irradiated using modulated curing methods at two C-factor levels. *Dent Mater* 24:392-398.

Dewaele M, Asmussen E, Peutzfeldt A, Munksgaard EC, Benetti AR, Finné G, *et al.* (2009). Influence of curing protocol on selected properties of light-curing polymers: degree of conversion, volume contraction, elastic modulus, and glass transition temperature. *Dent Mater* 25: 1576-1584.

Emami N, Söderholm KJ (2003). How light irradiance and curing time affect monomer conversion in light-cured resin composites. *Eur J Oral Sci* 111:536-542.

Feng L, Suh BI (2007). Exposure reciprocity law in photopolymerization of multi-functional acrylates and methacrylates. *Macromol Chem Phys* 208:295-306.

Halvorson RH, Erickson RL, Davidson CL (2002). Energy dependent polymerization of resin-based composite. *Dent Mater* 18:463-469.

Kanca J 3rd, Suh BI (1999). Pulse activation: reducing resin-based composite contraction stresses at the enamel cavosurface margins. *Am J Dent* 12:107-112.

Leprince J, Lamblin G, Truffier-Boutry D, Demoustier-Champagne S, Devaux J, Mestdagh M, *et al.* (2009). Kinetic study of free radicals trapped in dental resins stored in different environments. *Acta Biomater* 5:2518-2524.

Lovell LG, Newman SM, Bowman CN (1999). The effects of light intensity, temperature, and comonomer composition on the polymerization behavior of dimethacrylate dental resins. *J Dent Res* 78:1469-1476.

Lu H, Stansbury JW, Bowman CN (2005). Impact of curing protocol on conversion and shrinkage stress. *J Dent Res* 84:822-826.

Musanje L, Darvell BW (2003). Polymerization of resin composite restorative materials: exposure reciprocity. *Dent Mater* 19:531-541.

Ottaviani MF, Fiorini A, Mason PN, Corvaja C (1992). Electron spin resonance studies of dental composites: effects of irradiation time, decay over time, pulverization, and temperature variations. *Dent Mater* 8: 118-124.

Peutzfeldt A, Asmussen E (2005). Resin composite properties and energy density of light cure. *J Dent Res* 84:659-662.

Poshusta AK, Bowman CN, Anseth KS (2002). Application of a kinetic gelation simulation to the characterization of in situ cross-linking biomaterials. *J Biomater Sci Polym Ed* 13:797-815.

Price RB, Felix CA, Andreou P (2004). Effects of resin composite composition and irradiation distance on the performance of curing lights. *Biomaterials* 25:4465-4477.

Sakaguchi RL, Ferracane JL (2001). Effect of light power density on development of elastic modulus of a model light-activated composite during polymerization. *J Esthet Restor Dent* 13:121-130.

Soh MS, Yap AU, Siow KS (2004). Post-gel shrinkage with different modes of LED and halogen light curing units. *Oper Dent* 29:317-324.

Sustercic D, Cevc P, Funduk N, Pintar MM (1997). Determination of curing time in visible-light-cured composite resins of different thickness by electron paramagnetic resonance. *J Mater Sci Mater Med* 8:507-510.

Truffier-Boutry D, Gallez XA, Demoustier-Champagne S, Devaux J, Mestdagh M, Champagne B, *et al.* (2003). Identification of free radicals trapped in solid methacrylated resins. *J Polym Sci Part A: Polym Chem* 41:1691-1699.

Truffier-Boutry D, Demoustier-Champagne S, Devaux J, Biebuyck JJ, Mestdagh M, Larbanois P, *et al.* (2006). A physico-chemical explanation of the post-polymerisation shrinkage in dental resins. *Dent Mater* 22:405-412.

Zhu S, Tian Y, Hamielec AE, Eaton DR (1990). Radical concentrations in free radical copolymerization of MMA/EGDMA. *Polymer* 31: 154-159.

Reproduced with permission of the copyright owner. Further reproduction prohibited without permission.